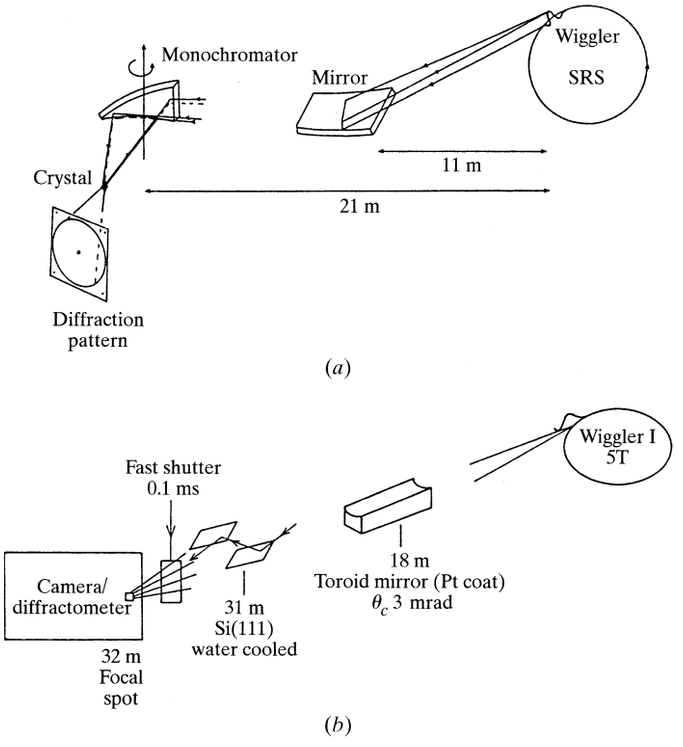

Figure 8.1.4.1
Common beamline optics modes. (*a*) Horizontally focusing cylindrical monochromator and vertical focusing mirror [shown here for station 9.6 as existed at the SRS (adapted from Helliwell *et al.*, 1986)]. (*b*) Rapidly tunable double-crystal monochromator and point-focusing toroid mirror [shown here as existed for station 9.5 at the SRS (adapted from Brammer *et al.*, 1988)].

(4) to provide a different polarization (*e.g.* to rotate the plane of polarization, to produce circularly polarized light *etc.*).

The classification of a periodic magnet ID as a wiggler or undulator is based on whether the angular deflection, δ, of the electron beam is small enough to allow radiation emitted from one pole to interfere directly with that from the next pole. In a wiggler, $\delta \gg \gamma^{-1}$, so the interference is negligible and the spectral emission (Fig. 8.1.2.2*a*) is very similar in shape to, but scaled up from, the universal curve (*i.e.* bending magnet spectral shape). In an undulator $\delta \leq \gamma^{-1}$ and the interference effects are highly significant (Fig. 8.1.2.2*b*). If the period of the ID is λ_u (cm), then the wavelengths λ_i (i integer) emitted are given by

$$\lambda_i = \frac{\lambda_u}{i2\gamma^2}\left(1 + \frac{K^2}{2} + \gamma^2\theta^2\right), \qquad (8.1.3.1)$$

where $K = \gamma\delta$.

The spectral width of each peak is

$$\Delta_i \simeq 1/iN, \qquad (8.1.3.2)$$

where N is the number of poles. The angular deflection, δ, is changed by opening or closing the gap between the pole pieces.

8.1.4. Beam characteristics delivered at the crystal sample

The sample acceptance, α [equation (8.1.4.1)], is a quantity to which the synchrotron machine emittance [equation (8.1.2.2)] should be matched, *i.e.*,

$$\alpha = x\eta, \qquad (8.1.4.1)$$

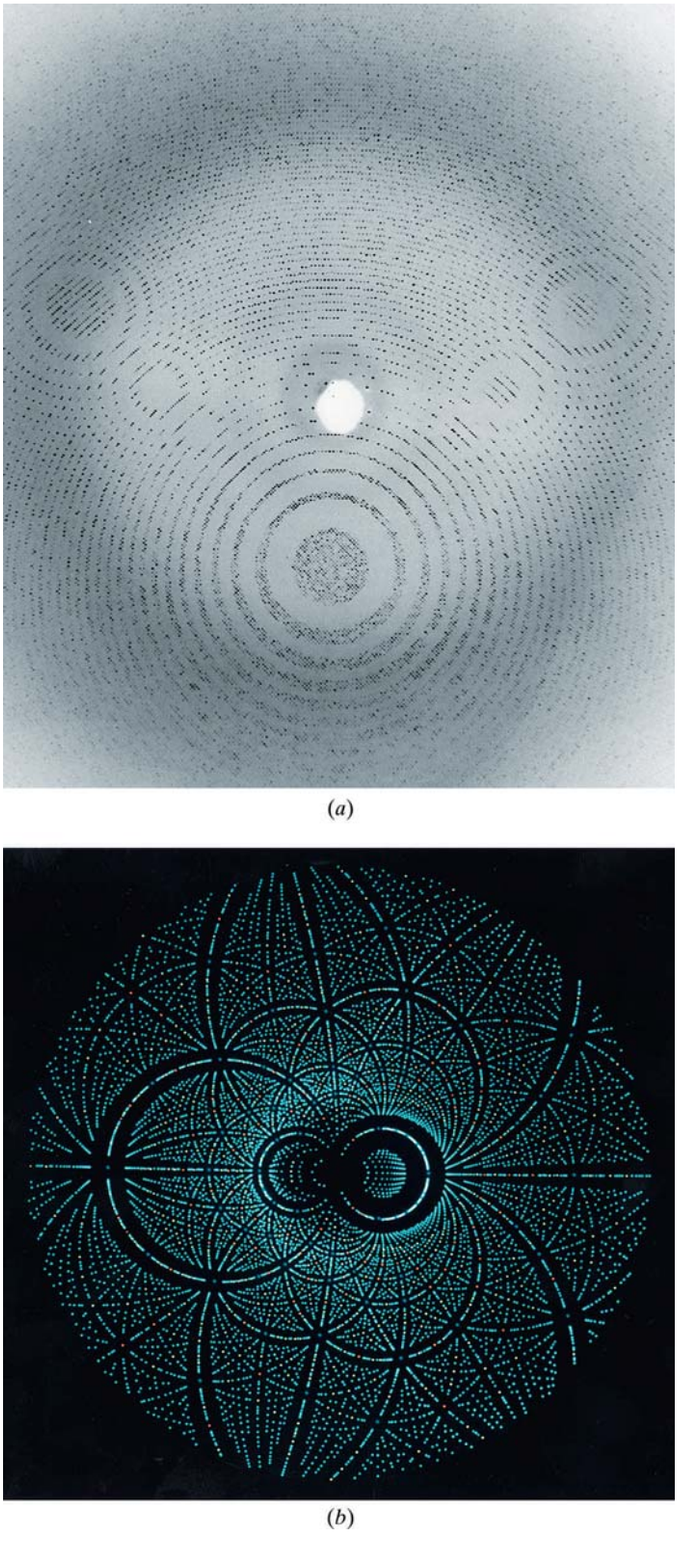

Figure 8.1.4.2
Single-crystal SR diffraction patterns. (*a*) Rhinovirus monochromatic oscillation photograph recorded at CHESS (Arnold *et al.* 1987; see also Rossmann & Erickson, 1983). (*b*) Prediction of a protein crystal Laue diffraction pattern (for an illuminating bandpass, without monochromator, $\sim 0.4 < \lambda < 2.6$ Å). The colour coding is according to the multiplicity of each spot: turquoise for singlet reflections, yellow for doublets, orange for triplets and blue for quartet or higher-multiplicity Laue spots (Cruickshank *et al.*, 1991).

where x is the sample size and η the mosaic spread. For example, if $x = 0.1$ mm and $\eta = 1$ mrad (0.057°), then $\alpha = 10^{-7}$ m rad or 100 nm rad.

Copyright © 2012 International Union of Crystallography

Table 8.1.4.1
Internet addresses of SR facilities with macromolecular crystallography beamlines

Synchrotron-radiation source	Location	Address
ALS, Advanced Light Source	Lawrence Berkeley Lab., Berkeley, California, USA	http://www-als.lbl.gov/als/
ANKA Synchrotron	Karlsruhe, Germany	http://ankaweb.fzk.de/
APS, Advanced Photon Source	Argonne National Lab., Chicago, Illinois, USA	http://epics.aps.anl.gov/
Australian Synchrotron	Clayton, Victoria, Australia	http://www.synchrotron.org.au/
BESSY	Berlin, Germany	http://www.bessy.de/
Brazilian Synchrotron Light Laboratory	Campinas, Brazil	http://www.lnls.br/
BSRF, Beijing Synchrotron Radiation Facility	Beijing, China	http://www.ihep.ac.cn/bsrf/english/main/main.htm
CAMD, Center for Advanced Microstructures and Devices	Baton Rouge, Louisiana, USA	http://www.camd.lsu.edu/
Canadian Light Source	Saskatoon, Canada	http://www.lightsource.ca/
CHESS, Cornell High Energy Synchrotron Source	Ithaca, New York, USA	http://www.chess.cornell.edu/
Diamond Light Source	Harwell Science and Innovation Campus, Didcot, England	http://www.diamond.ac.uk/
Elettra	Trieste, Italy	http://www.elettra.trieste.it
ESRF, European Synchrotron Radiation Facility	Grenoble, France	http://www.esrf.fr/
HASYLAB DESY, Deutsches Elektronen-Synchrotron	Hamburg, Germany	http://www.desy.de/
Kurchatov Center for Synchrotron Radiation and Nanotechnology	Moscow, Russian Federation	http://www.kcsr.kiae.ru/en/
LNLS, National Synchrotron Light Laboratory	Campinas, Brazil	http://www.lnls.br/
MAXLab (see also MAX IV project)	Lund, Sweden	http://www.maxlab.lu.se/, http://www.maxlab.lu.se/maxlab/max4/index.html
NSLS, National Synchrotron Light Source (see also NSLS II; under construction)	Brookhaven National Lab., New York, USA	http://www.nsls.bnl.gov/, http://www.bnl.gov/nsls2/
The Photon Factory, KEK	Tsukuba, Japan	http://pfwww.kek.jp/
PLS, Pohang Light Source	Pohang, Korea	http://pal.postech.ac.kr/
SESAME (Synchrotron-light for Experimental Science and Applications in the Middle East)	Allan, Jordan	http://www.sesame.org.jo/
Shanghai Synchrotron Radiation Facility	Shanghai, China	http://ssrf.sinap.ac.cn/english/1/Introduction.htm
SLS, Swiss Light Source	Paul Scherrer Institut, Villigen, Switzerland	http://sls.web.psi.ch/view.php/about/index.html
Soleil	Gif-sur-Yvette, Paris, France	http://www.synchrotron-soleil.fr/portal/page/portal/Accueil
SPring-8, Super Photon Ring	Riken Go, Japan	http://www.spring8.or.jp/
SRRC, Synchrotron Radiation Research Center	Hsinchu City, Taiwan	http://www.nsrrc.org.tw/
SSRL, Stanford Synchrotron Radiation Laboratory	SLAC, California, USA	http://www-ssrl.slac.stanford.edu/
VEPP-3	Novosibirsk, Russia	http://ssrc.inp.nsk.su/

At the sample position, the intensity of the beam, usually focused, is a useful parameter:

$$\text{Intensity} = \text{photons per s per focal spot area.} \qquad (8.1.4.2)$$

Moreover, the horizontal and vertical convergence angles are ideally kept smaller than the mosaic spread, *e.g.* ~1 mrad, so as to measure reflection intensities with optimal peak-to-background ratio.

Producing a focal spot area that is approximately the size of a typical crystal (~0.1 mm) and with a convergence angle ~1 mrad sets a sample acceptance requirement to be met by the X-ray beam and machine emittance. A machine with an emittance that matches the acceptance of the sample greatly assists the simplicity and performance of the beamline optics (mirror and/or monochromator) design. The common beamline optics schemes are shown in Fig. 8.1.4.1.

In addition to the focal spot area and convergence angles, it is necessary to provide the appropriate spectral characteristics. In monochromatic applications, involving the rotating-crystal diffraction geometry, for example, a particular wavelength, λ, and narrow spectral bandwidth, $\delta\lambda/\lambda$, are used. Fig. 8.1.4.2(*a*) shows an example of a monochromatic oscillation diffraction photograph from a rhinovirus crystal as an example recorded at CHESS, Cornell. Fig. 8.1.4.2(*b*) shows the prediction of a white-beam broad-band Laue diffraction pattern from a protein crystal that was recorded at the SRS wiggler, Daresbury, colour-coded for multiplicity.

Table 8.1.4.1 lists the internet addresses of the SR facilities worldwide that currently have macromolecular beamlines. A considerable suite of information on SR and free electron laser (FEL) sources can also be found at http://www.lightsources.org/cms/. Comprehensive statistics for the macromolecular crystal structures from all the various beamlines over the years can be obtained at http://biosync.rcsb.org/.

8.1.5. Evolution of SR machines and experiments

8.1.5.1. First-generation SR machines

The so-called first generation of SR machines were those which were parasitic on high-energy physics operations, such as DESY in Hamburg, SPEAR in Stanford, NINA in Daresbury and VEPP in Novosibirsk. These machines had high fluxes into the X-ray range and enabled pioneering experiments. Parratt (1959) discussed the use of the CESR (Cornell Electron Storage Ring) for X-ray diffraction and spectroscopy in a very perceptive paper. Cauchois *et al.* (1963) conducted *L*-edge absorption spectroscopy at Frascati and were the first to diffract SR with a crystal (quartz). The opening experimental work in the area of biological diffraction was by Rosenbaum *et al.* (1971). In protein crystallography, multiple-wavelength anomalous-dispersion effects (Fig.